Solid-State Displacement Synthesis of Alkaline-Earth Selenide for White Emission through Alternating Current Electroluminescence

Wang, Yanze; Suo, Hao; Zhang, Xin; Chun, Fengjun; Shen, Junda; Chen, Bing; Zheng, Weilin; Xing, Zhifeng; Wei, Han-Lin; Li, Yang Yang; Wang, Feng

Published in:
ACS Materials Letters

Published: 05/12/2022

Document Version:
Post-print, also known as Accepted Author Manuscript, Peer-reviewed or Author Final version

Published version (DOI):
10.1021/acsmaterialslett.2c00919

Publication details:
Wang, Y., Suo, H., Zhang, X., Chun, F., Shen, J., Chen, B., Zheng, W., Xing, Z., Wei, H.-L., Li, Y. Y., & Wang, F. (2022). Solid-State Displacement Synthesis of Alkaline-Earth Selenide for White Emission through Alternating Current Electroluminescence. *ACS Materials Letters*, *4*(12), 2447-2453. https://doi.org/10.1021/acsmaterialslett.2c00919

Solid-state displacement synthesis of alkaline-earth selenide for white emission through alternating current electroluminescence

Yanze Wang[§†], Hao Suo[§†], Xin Zhang[§†], Fengjun Chun[§†], Junda Shen[§], Bing Chen[§†], Weilin Zheng[§†], Zhifeng Xing[§†], Han-Lin Wei[§†], Yang Yang Li[§], and Feng Wang[§†*]

[§]Department of Materials Science and Engineering, City University of Hong Kong, 83 Tat Chee Avenue, Kowloon 999077, Hong Kong SAR, China.

[†]City University of Hong Kong Shenzhen Research Institute, Shenzhen 518057, China.

* Corresponding author: fwang24@cityu.edu.hk (F.W.)

Abstract: Alkaline-earth selenides (AESe) are functional materials of both fundamental and technological importance, but their chemical synthesis has met with limited success. Herein, a solid-state displacement reaction is described for the rapid synthesis of various AESe crystals without the need for hazardous chemicals. The reaction mechanism is studied by careful control of the experimental variables such as the reaction temperature (800-1400 °C), atmospheres (air, N_2, and N_2/H_2 mixture), and Se precursors (ZnSe and Se). Using $AECO_3$ and ZnSe (ZnS) as precursor materials under N_2/H_2 mixture atmosphere, we synthesized a series of AESe, AES, and AE(S,Se) crystals with high crystallinities. Doping of luminescent lanthanide ions such as Eu^{2+} is concomitantly achieved during the synthesis, yielding tunable photoluminescence that is useful for constructing white light-emitting devices in combination with electroluminescent ZnS:Cu.

Alkaline-earth selenides (AESe, AE = Ca, Sr, and Ba) are an important class of functional materials that provide many research topics in solid-state physics, chemistry, and materials science. Owing to their stable structure and semiconducting behavior, AESe crystals have found applications in optical storage, X-ray imaging, and lighting devices.[1-4] Compared with other kinds of selenides such as CdSe, AESe features low fabrication cost, high luminous efficiency, and large doping capacity for various impurity ions such as lanthanides for precise optical tuning.[5-6] Despite the attractive characteristics, the potentials of AESe are largely unexploited due to the difficulties in the rapid and environmentally benign synthesis of AESe crystals.

Several synthetic protocols have been described to prepare AESe crystals in previous reports, such as hydrothermal synthesis,[7] co-precipitation,[8] solid-state reaction,[9] and solid-phase diffusion.[10] However, these methods typically suffer from complicated fabrication processes, low product yields, and/or hazardous synthesis conditions. In a classic synthesis of SrSe developed by Asano and co-workers,[11] for example, $SrSeO_4$ raw materials needed to be calcined under a mixture gas stream of H_2/H_2Se for 50 min followed by post-annealing at 1000 °C under N_2 gas stream for another 1 h. To realize Pb^{2+} doping, the resulting product needed further calcination with PbS at 1000 °C under N_2 gas stream for 40 min. Therefore, it is imperative to develop simple and efficient synthetic methods for the rapid preparation of high-quality AESe crystals.

In this study, we describe a solid-state displacement method for the efficient synthesis of AESe crystals with tunable compositions. The principle of the synthetic protocol is elaborately studied by systematical variation of the reaction conditions. By using different precursors materials, we establish a rapid synthesis of a family of alkaline-earth chalcogenides, including AESe, AES, and alloyed AE(S,Se) crystals. Furthermore, luminescent lanthanide ions are incorporated into the crystals and the resultant phosphors are exploited as spectral converters in ZnS-based alternating-current electroluminescence (ACEL) devices for white emissions.

Our synthesis employed $AECO_3$ and ZnSe as the raw materials, which were chosen for economical and safety considerations. A quartz tube furnace was used for the sample preparations (**Figure 1a**). To avoid the formation of solid byproducts that may contaminate the desired AESe crystals, we conducted the reaction in a reducing atmosphere consisting of H_2 (10 vol%) in N_2. Due to the existence of H_2, the synthesis is expected to proceed according to the following reaction:[12]

$$AECO_3 \rightarrow AEO + CO_2 \uparrow \quad (1)$$

$$AEO + ZnSe \rightarrow AESe + ZnO \quad (2)$$

$$ZnO + H_2 \rightarrow Zn \uparrow + H_2O \uparrow \quad (3)$$

Since the boiling point of monomeric Zn is about 907 °C,[13] all the byproducts are readily evaporated during the high-temperature synthesis, leaving behind the final product with high purity.

As an explanatory experiment, we synthesized CaSe using $CaCO_3$ and ZnSe as the raw materials. **Figure 1b** shows the X-ray diffraction (XRD) pattern of a typical sample synthesized at 1200 °C for 1 h. All the diffraction peaks can be well indexed in accord with cubic phase CaSe (JCPDS file number 77-2012), suggesting high purity and crystallinity of the product.[14] The sample was further characterized by scanning electron microscopy (SEM), revealing an irregular particle shape with an average size of about 25 μm (**Figure 1c**). The energy-dispersive X-ray spectroscopy (EDX) mapping of a randomly selected particle demonstrates the uniform distribution of the constituent Ca and Se elements across the particle.

The proposed reaction mechanism was supported by detecting metallic Zn in the byproduct collected from the surface of the alumina adiabatic plug at the outlet side of the quartz tube (**Figure 1d**). The transformation of ZnO into Zn and H_2O under

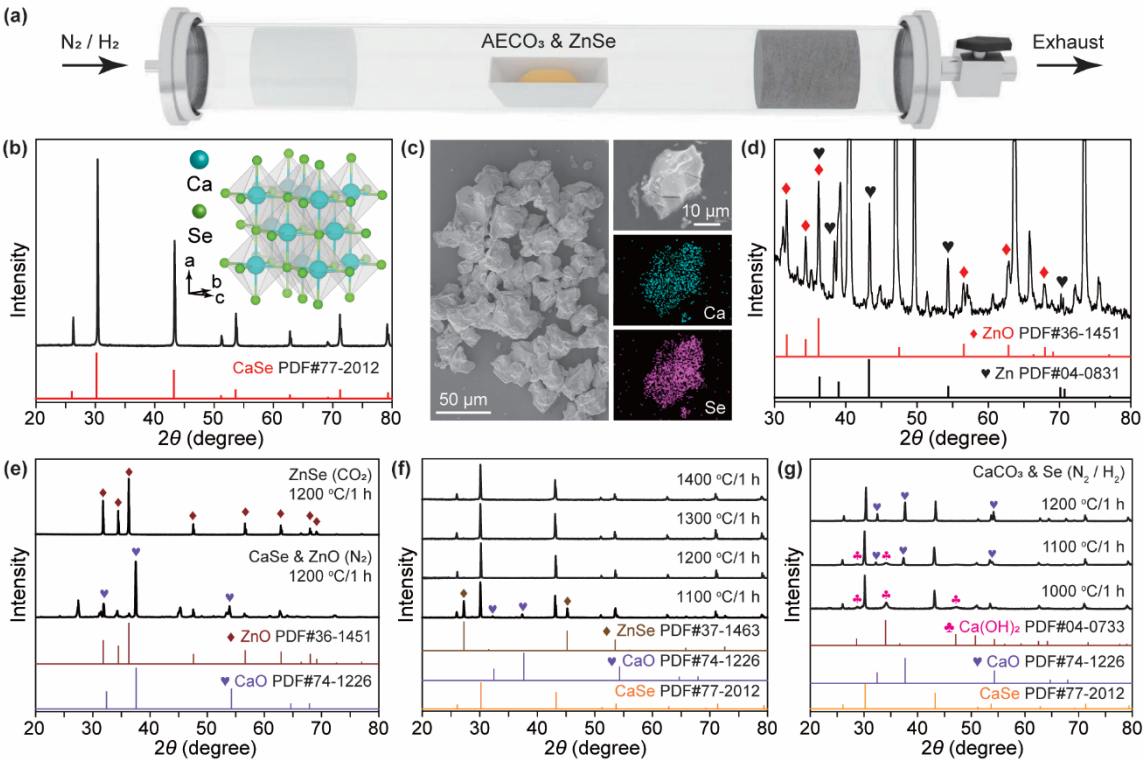

Figures 1. (a) Schematic illustration of synthesis setup. (b) XRD pattern of CaSe crystals synthesized by calcination at 1200 °C for 1 h in the N_2/H_2 mixture atmosphere. Inset: crystal structure of the CaSe crystals. (c) SEM image of the as-synthesized CaSe crystals and related EDX mapping of a single CaSe particle. (d) XRD pattern of the byproduct collected from the alumina adiabatic plug at the outlet side. (e) XRD patterns of ZnSe calcined at 1200 °C for 1 h under CO_2 (top panel) and N_2 with ZnO (bottom panel). (f) XRD patterns of the products synthesized at different temperatures in the N_2/H_2 mixture atmosphere for 1 h. (g) XRD pattern of the products synthesized using Se powder as the raw material at different temperatures in the N_2/H_2 mixture atmosphere for 1 h.

the N_2/H_2 mixture atmosphere was further verified by observing the complete volatilization of solid ZnO upon heating at 1200 °C (**Figure S1**). Note that the ZnO component detected in the residue (**Figure 1d**) was probably formed due to partial oxidation of the Zn elements as the evaporated byproducts flew towards the outlet.[15]

In addition to facilitating the removal of ZnO byproduct, the H_2 component in the reaction atmosphere is also essential for enabling the synthesis.[11-12, 16] In the absence of H_2, ZnSe tends to oxidize into ZnO due to CO_2 evolved from $CaCO_3$ (**Figure 1e**, top panel), thereby suppressing the reaction at the source. H_2 also pushes the displacement reaction (**Eqn. 2**) forward by continuously removing ZnO byproducts from the system. Our control experiments showed that CaSe could be converted back into CaO upon reaction with ZnO in the N_2 atmosphere at 1200 °C (**Figure 1e**, bottom panel).

We next investigated the temperature and time effects on the reaction. According to the XRD characterizations (**Figure 1f**), pure phase CaSe crystals were obtained in a wide temperature range of 1200-1400 °C, indicating the high thermal stability of the product.[17] As the reaction temperature dropped to 1100 °C, heterogeneous phases comprising ZnSe and CaO impurities were detected due to the incomplete reaction. Notably, the ZnSe and CaO impurities can hardly be eliminated by prolonging the reaction time to 10 h (**Figure S2a**), suggesting that a relatively high temperature is indispensable to facilitate the displacement reaction. It is worth noting that short calcination times (< 0.5 h) at 1200 °C would also lead to incomplete reactions (**Figure S2b**). While extended calcination for overlong

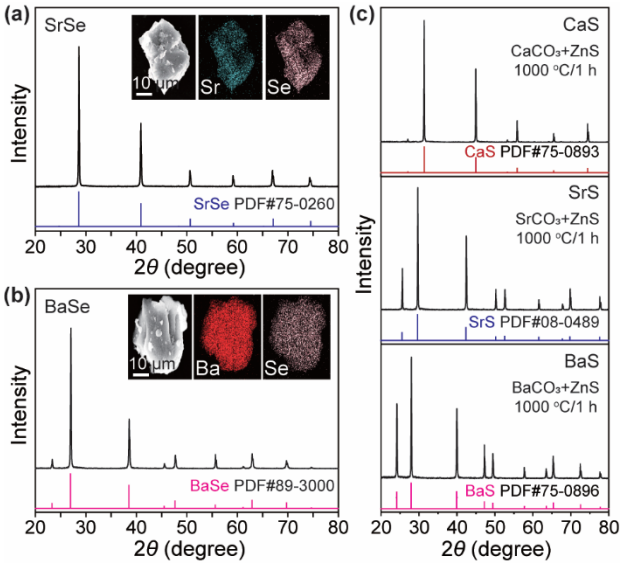

Figures 2. (a, b) XRD patterns of SrSe and BaSe crystals synthesized at 1000 °C for 1 h in the N_2/H_2 mixture atmosphere, respectively. Inset: SEM images and related EDX elemental mapping of randomly selected SrSe and BaSe particles, respectively. (c) XRD patterns of CaS, SrS, and BaS samples synthesized at 1000 °C for 1 h in the N_2/H_2 mixture atmosphere, respectively.

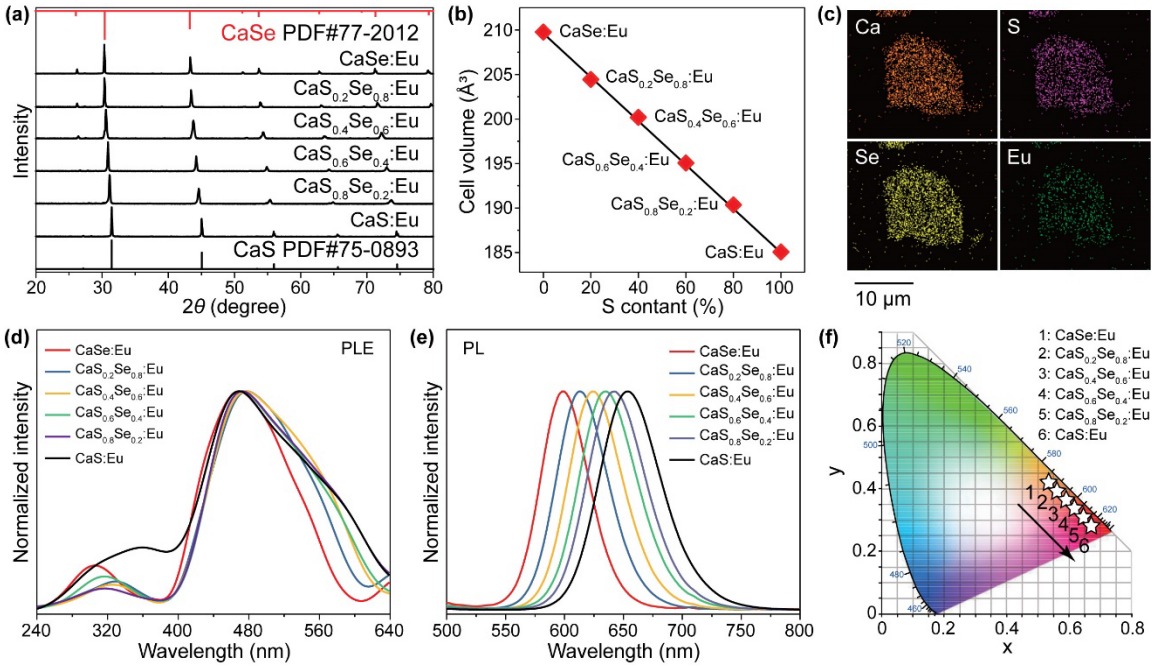

Figures 3. (a) XRD patterns of $CaS_xSe_{(1-x)}:Eu^{2+}$ (1%, x=0, 0.2, 0.4, 0.6, 0.8, 1) crystals synthesized at 1200 °C for 1 h in the N_2/H_2 mixture atmosphere. (b) The cell volume of the $CaS_xSe_{(1-x)}$ samples as a function of x value derived from the XRD patterns. (c) EDX mapping of a typical particle composed of $CaS_{0.6}Se_{0.4}:Eu^{2+}$ (1%). (d,e) Normalized PLE and PL spectra of the as-synthesized $CaS_xSe_{(1-x)}:Eu^{2+}$. (f) Commission Internationale de l'Eclairage (CIE) chromaticity coordinates of the multicolor emissions from the samples shown in (e). The chromaticity coordinates of samples #1-6 were (0.529, 0.427), (0.562, 0.391), (0.583, 0.377), (0.610, 0.335), (0.648, 0.315), and (0.667, 0.282), respectively.

time (> 4 h) could result in softening of the product, making it difficult to collect after cooling.

The selection of selenium source is also important for the synthesis. By calcining $CaCO_3$ with pure Se powder at different temperatures for 1 h with other conditions kept constant, significant amounts of oxide and hydroxide byproducts [i.e., $Ca(OH)_2$ and CaO] emerged according to the XRD patterns (**Figure 1g**). The observations were ascribed to incomplete displacement reactions caused by evaporation loss of the Se precursors, stemming from the low boiling temperature of Se power (~685 °C).[18-19] Notably, when $CaCO_3$ and Se powder was calcined in the pure N_2 atmosphere, the final product was dominated by CaO with no detectable CaSe (**Figure S3**). The results suggest that H_2 plays an essential role in initiating this selenization process by reducing monomeric Se into Se^{2-} ions.

The synthetic protocol can be readily extended to prepare other types of alkaline-earth chalcogenides. For example, by calcining $SrCO_3$ and $BaCO_3$ with ZnSe in the same way, we obtained pure cubic phase SrSe and BaSe, respectively (**Figures 2a** and **b**).[20-21] Furthermore, pure cubic phase CaS, SrS, and BaS were synthesized by calcining the relevant alkaline-earth carbonates with ZnS (**Figure 2c**).[22] Similar to the preparation of CaSe, these syntheses can all be accomplished over a large temperature range (around 1000-1400 °C) under the N_2/H_2 mixture atmosphere (**Figures S4** and **S5**). As the reaction atmosphere or chalcogen source was changed, pure-phase alkaline-earth chalcogenides could no longer be obtained (**Figures S6**).

In the further set of experiments, we demonstrated the synthesis of alloyed Ca(S,Se) crystals by using mixture precursors of ZnSe and ZnS at controlled ratios. This compositional engineering permits precise control over the crystal field in the host lattice, which can be harnessed to tune the optical emission of impurity dopants such as lanthanide ions.[6, 12, 23-24] Specifically, we synthesized a series of $CaS_xSe_{(1-x)}$ (x=0, 0.2, 0.4, 0.6, 0.8, 1) crystals doped with 1 % of Eu^{2+} by including EuF_2 in the precursor materials. The XRD patterns in **Figure 3a** reveal the single phase of the crystal with gradually evolving lattice constants. By Rietveld refinement of the XRD patterns of the $CaS_xSe_{(1-x)}$ crystals, we detected a linear decrease in the unit-cell volume with the increase of S content (**Figure 3b** and **Figures S7**). The results confirmed the successful substitution of S^{2-} ions for larger Se^{2-} (1.84 versus 1.98 Å; coordination number = 6) that caused contraction of the crystal lattice according to Vegard's law.[12, 16, 25] EDX mapping of a typical sample composed of $CaS_{0.6}Se_{0.4}:Eu^{2+}$ further verified the presence of the constituent elements of Ca, S, Se, and Eu that were uniformly distributed across the crystal (**Figure 3c**). And the calculated atomic ratios were consistent with the designed crystal compositions (**Figures S8** and **Table S1**).

The photoluminescence excitation (PLE) and photoluminescence (PL) properties of the $CaS_xSe_{(1-x)}:Eu^{2+}$ crystals were shown in **Figures 3d-e**. All samples exhibited two excitation peaks at around 320 and 470 nm (**Figure 3d**), which were assigned to the host absorption (~320 nm) and $4f^7$ ($^8S^{7/2}$)→$4f^65d^1$ transition of the Eu^{2+} (470 nm), respectively.[26-28] The emission spectrum under excitation of 470 nm exhibits the characteristic Eu^{2+} band centered at ~600 nm owing to the $4f^65d^1$→$4f^7$ transition (**Figure 3e**).[29] As the S^{2-} concentration in the crystals increased from 0 to 100 %, the emission peak was redshifted from 598 to 654 nm, corresponding to a color change from orange to deep red as shown in CIE chromaticity coordinate diagram (**Figure 3f**). The spectral shift was ascribed to S-induced increase of the crystal-field strength, which enhanced splitting of the Eu^{2+} 5*d* level.[25-26, 30] By changing the coordination environment of Eu^{2+}, S alloying also resulted in an increase of the quantum yields from 12.44 to 46.21 % (**Table S2**).

The alloyed Ca(S,Se):Eu^{2+} crystals with broad and tunable emissions appeal to lighting applications, especially for composing white light in combination with devices emitting in the

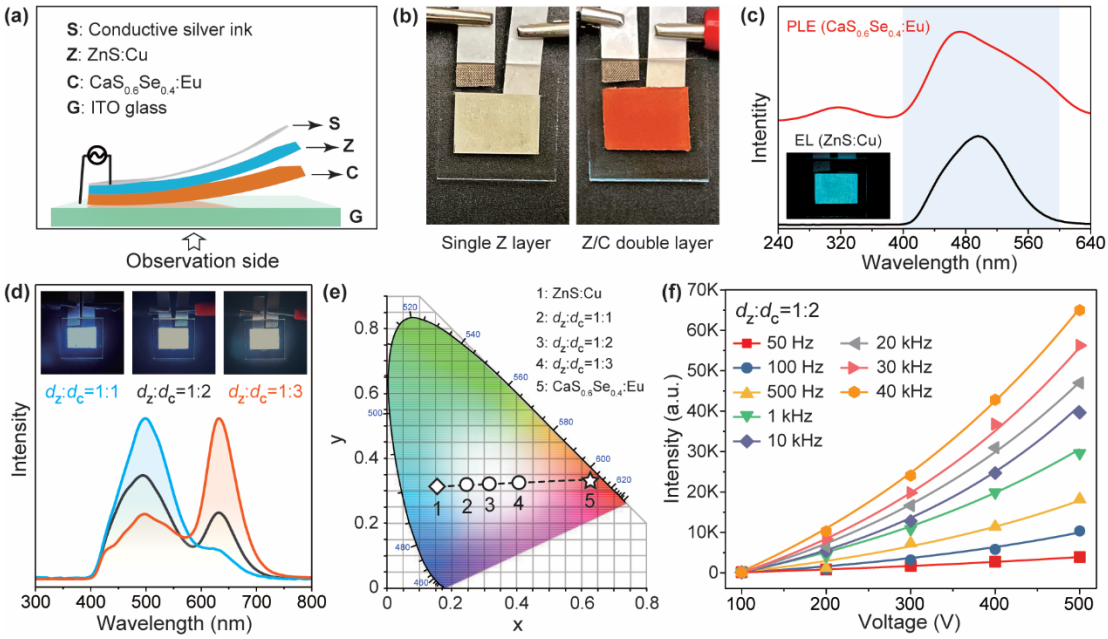

Figures 4. (a) Schematic diagram of the ACEL device. (b) Photographs the as-fabricated device comprising a single Z layer and Z/C double layers, respectively. (c) Comparison of the photoluminescence excitation (PLE) spectra of $CaS_{0.6}Se_{0.4}:Eu^{2+}$ (monitored at 635 nm) and the electroluminescence (EL) emission spectra of ZnS:Cu. The insets show EL image of the ACEL device comprising a single Z layer tested at 300 V/10 kHz. (d) Emission spectra of Z/C double layers devices with d_Z:d_C of 1:1, 1:2, and 1:3, respectively. Inset: corresponding images of the device showing cool, normal, and warm white light emissions, respectively. (e) CIE chromaticity coordinates of the white light emissions from the ACEL devices shown in (c) and (d). The color coordinates of the samples #1-4 were: (0.159, 0.320), (0.240, 0.324), (0.321, 0.328), and (0.410, 0.332), respectively. For reference, the color coordinate of photoluminescence from $CaS_{0.6}Se_{0.4}:Eu^{2+}$ (0.610, 0.335) is also shown. (f) Integrated luminescence intensity of the ACEL device with d_Z:d_C of 1:2 at different application voltages and frequencies.

short wavelength.[24, 26, 31] As a proof of concept, we devised a white alternating current electroluminescence (ACEL) device by combining commercially available ZnS:Cu with $CaS_{0.6}Se_{0.4}:Eu^{2+}$ on account of their complementary emission colors. **Figure 4a** depicts the schematic design of the device in our study, which featured a stacked configuration comprising a silver ink conductive top (S), a ZnS:Cu EL layer (Z), a $CaS_{0.6}Se_{0.4}:Eu^{2+}$ phosphor layer (C), and an ITO glass substrate (G). **Figure 4b** shows the photographs of typical ACEL devices comprising a single Z layer and Z/C double layers observed through the G layer. The EL emission peak of ZnS:Cu at ~500 nm was reasonably resonant with the $4f^7$ to $4f^65d^1$ transition of Eu^{2+} in $CaS_{0.6}Se_{0.4}:Eu^{2+}$ (**Figure 4c**), which ensures efficient energy transfer for the construction of phosphor-converted ACEL.[32-34]

Figure 4d shows the emission spectra of the ACEL devices comprising Z/C double layers tested at 300 V/10 kHz. By fixing the Z layer (d_Z, ~30 μm) and gradually increasing the thickness of the C layer (d_C, ~30-90 μm) (**Figures S9**), we realized precise control over the emission intensity balance of the two layers, demonstrating emission fine-tuning from greenish-blue to white and then to warm white (**Figure 4e**). The corresponding color-conversion efficiencies (η_{CCE}) were estimated using the following equation:[35-36]

$$\eta_{CCE} = \frac{I_C}{I_{Z/CSS} - I_Z} \quad (4)$$

where I_C and I_Z are the emission intensities of C and Z components in the Z/C double-layer devices, and $I_{Z/CSS}$ is the emission intensity of the reference devices composed of ZnS:Cu and inert $CaS_{0.6}Se_{0.4}$ (**Figures S10**). The calculated η_{CCE} were about 9.2, 16.7, and 22.6 % at a d_Z:d_C of 1:1, 1:2, and 1:3, respectively.

We detected a drop in device brightness with the increase of d_C, owing to the decreased electric field.[37-38] Specifically, we recorded luminance of 17.65, 10.44, and 2.81 cd m^{-2} for devices with a d_C of about 30, 60, and 90 μm, respectively. The brightness is comparable to the screen of a smart sports bracelet (21.46 cd m^{-2} at 50 % brightness). The luminous efficiency for devices with a d_C of about 30, 60, and 90 μm was further determined to be 10.51, 6.24, and 1.67 cd $(W{\cdot}m^2)^{-1}$, respectively. The reduction of luminous efficiency in thick devices was ascribed to increased loss of light transmittance.[39]

We further characterized the device with a d_C of 60 μm that exhibited white emissions. **Figure 4f** shows the emission intensity of the device as a function of applied voltages in the 100-500 V range at different frequencies (see **Figures S11** for the corresponding spectra). As shown in **Figure 4f**, the device can be well lit up by excitation of ~200 V at a frequency of 50 Hz. Moreover, the luminescence intensity of the device showed an exponential growth trend with increasing voltage and frequency, similar to that of the single Z layer device due to the Z-to-C energy transfer mechanism (**Figures S12**).[40-43] Notably, the emission peak of ZnS:Cu showed a blue shift with increasing frequency due to the peculiarity of the ZnS:Cu energy level structure, which comprises two different acceptor states.[44] This effect permits additional control over the color output of the device (**Figure S13**).

In conclusion, we have developed a new synthetic protocol for the preparation of alkaline-earth selenides and sulfides. The synthesis involves the calcination of alkaline-earth carbonates with ZnSe and ZnS in a reducing atmosphere consisting of H_2 (10 vol%) in N_2, which is simple, efficient, and environmentally benign. Notably, the synthesis permits concomitant doping of impurity ions such as luminescent lanthanides, generating tun-

able optical emissions. Accordingly, we have established a phosphor-converted ACEL device consisting of ZnS:Cu as the EL layer for white light emissions. Our findings would enrich the library of doped semiconductor materials and inspire new ideas of synthesizing difficult-to-produce compounds.

ASSOCIATED CONTENT

Supporting Information
The Supporting Information is available free of charge at https://pubs.acs.org.
Synthesis, XRD patterns, SEM images, Rietveld refinement of XRD patterns, PL, and EL spectra.

AUTHOR INFORMATION

Corresponding Author

* **Feng Wang** – *Department of Materials Science and Engineering, City University of Hong Kong, Kowloon 999077 Hong Kong SAR, China; City University of Hong Kong Shenzhen Research Institute, Shenzhen 518057, China; orcid.org/0000-0001-9471-4386; Email: fwang24@ cityu.edu.hk*

Authors

Yanze Wang – Department of Materials Science and Engineering, City University of Hong Kong, Kowloon 999077 Hong Kong SAR, China; City University of Hong Kong Shenzhen Research Institute, Shenzhen 518057, China; orcid.org/0000-0002-6001-8240

Hao Suo – Department of Materials Science and Engineering, City University of Hong Kong, Kowloon 999077 Hong Kong SAR, China; City University of Hong Kong Shenzhen Research Institute, Shenzhen 518057, China

Xin Zhang – Department of Materials Science and Engineering, City University of Hong Kong, Kowloon 999077 Hong Kong SAR, China; City University of Hong Kong Shenzhen Research Institute, Shenzhen 518057, China

Fengjun Chun – Department of Materials Science and Engineering, City University of Hong Kong, Kowloon 999077 Hong Kong SAR, China; City University of Hong Kong Shenzhen Research Institute, Shenzhen 518057, China

Bing Chen – Department of Materials Science and Engineering, City University of Hong Kong, Kowloon 999077 Hong Kong SAR, China; City University of Hong Kong Shenzhen Research Institute, Shenzhen 518057, China; orcid.org/0000-0002-0663-1343

Junda Shen – Department of Materials Science and Engineering, City University of Hong Kong, Kowloon 999077 Hong Kong SAR, China; orcid.org/0000-0003-4466-7221

Weilin Zheng – Department of Materials Science and Engineering, City University of Hong Kong, Kowloon 999077 Hong Kong SAR, China; City University of Hong Kong Shenzhen Research Institute, Shenzhen 518057, China; orcid.org/0000-0002-8270-3599

Zhifeng Xing – Department of Materials Science and Engineering, City University of Hong Kong, Kowloon 999077 Hong Kong SAR, China; City University of Hong Kong Shenzhen Research Institute, Shenzhen 518057, China

Han-Lin Wei – Department of Materials Science and Engineering, City University of Hong Kong, Kowloon 999077 Hong Kong SAR, China; City University of Hong Kong Shenzhen Research Institute, Shenzhen 518057, China

Yang Yang Li – Department of Materials Science and Engineering, City University of Hong Kong, Kowloon 999077 Hong Kong SAR, China; orcid.org/0000-0003-4153-9558

Author Contributions

The manuscript was written through the contributions of all authors.

ACKNOWLEDGMENT

The work described in this paper was substantially supported by a fellowship award from the Research Grants Council of the Hong Kong Special Administrative Region, China (Project No. CityU RFS2021-1S03).

REFERENCES

(1) Primak, W.; Kaufman, H.; Ward, R. X-ray diffraction studies of systems involved in the preparation of alkaline earth sulfide and selenide phosphors. *J. Am. Chem. Soc.* **1948**, 70, 2043-2046.

(2) Huang, X.; Yang, S. H.; Liu, W. L.; Guo, S. P. Noncentrosymmetric $Ba_6In_2Q_{10}$ (Q = S, Se): structural chemistry and nonlinear-optical activity. *Inorg. Chem.* **2021**, 60, 16932–16936.

(3) Li, Y. N.; Chen, Z. X.; Yao, W. D.; Tang, R. L.; Guo, S. P. Heterovalent cations substitution to design asymmetric chalcogenides with promising nonlinear optical performances. *J. Mater. Chem. C* **2021**, 9, 8659-8665.

(4) Li, Y. N.; Chi, Y.; Sun, Z. D.; Xue, H. G.; Suen, N. T.; Guo, S. P. Partial substitution induced centrosymmetric to noncentrosymmetric structure transformation and promising second-order nonlinear optical properties of $(K_{0.38}Ba_{0.81})Ga_2Se_4$. *Chem. Commun.* **2019**, 55, 13701-13704.

(5) Smith, A. L.; Rosenstein, R.; Ward, R. The preparation of strontium selenide and its properties as a base material for phosphors stimulated by infrared. *J. Am. Chem. Soc.* **1947**, 69, 1725-1729.

(6) Ahmadian, F.; Salary, A. First-principles study on the structural, electronic, and optical properties of $Ca_{1-x}Sr_xSe$ alloys. *J. Korean Phys. Soc.* **2016**, 68, 227-237.

(7) Kumar, N.; Kumar, V.; Swart, H.; Mishra, A. K.; Ngila, J. C.; Parashar, V. Controlled microstructural hydrothermal synthesis of strontium selenides host matrices for Eu^{II} and Eu^{III} luminescence. *Mater. Lett.* **2015**, 146, 51-54.

(8) Wang, J.; Zhu, Y.; Grimes, C. A.; Cai, Q. Multicolor lanthanide-doped CaS and SrS near-infrared stimulated luminescent nanoparticles with bright emission: application in broad-spectrum lighting, information coding, and bio-imaging. *Nanoscale* **2019**, 11, 12497-12501.

(9) Asano, S.; Yamashita, N.; Ogawa, Y. Luminescence et structure vibrationnelle des luminophores $CaS:Ce^{3+}$ et $CaSe:Ce^{3+}$. *Phys. Status Solidi B* **1983**, 118, 89-100.

(10) Vij, A.; Singh, S.; Kumar, R.; Lochab, S.; Kumar, V.; Singh, N. Synthesis and luminescence studies of Ce doped SrS nanostructures. *J. Phys. D: Appl. Phys.* **2009**, 42, 105103.

(11) Yamashita, N.; Ohira, T.; Mizuochi, H.; Asano, S. Luminescence of Pb^{2+} centers in SrS and SrSe phosphors. *J. Phys. Soc. Jpn.* **1984**, 53, 419-426.

(12) Yamashita, N.; Harada, O.; Nakamura, K. N. K. Photoluminescence spectra of Eu^{2+} centers in Ca(S, Se):Eu and Sr(S, Se):Eu. *Jpn. J. Appl. Phys.* **1995**, 34, 5539.

(13) Mewes, J. M.; Schwerdtfeger P. Exclusively relativistic: periodic trends in the melting and boiling points of group 12. *Angew. Chem. Int. Ed.* **2021**, 60, 7703-7709.

(14) Wang, Y. Z.; Chen, B.; Zhang, X.; Suo, H.; Zheng, W. L.; Shen, J. D.; Li, Y. Y.; Wang, F. Doubly doped BaZnOS microcrystals for multicolor luminescence switching. *Adv. Opt. Mater.* **2022**, 10, 2102430.

(15) Khanlary, M. R.; Vahedi, V.; Reyhani, A. Synthesis and characterization of ZnO nanowires by thermal oxidation of Zn thin films at various temperatures. *Molecules* **2012**, 17, 5021-5029.

(16) Zhang, J.; Wang, J.; Yu, R.; Yuan, H.; Su, Q. Luminescence properties of $Ca_{1-x}Sr_xSe$:Ce phosphors and their potential application for GaN-based LEDs. *Mater. Res. Bull.* **2009**, 44, 1093-1096.

(17) Lee, Y.; Lo, S. H.; Androulakis, J.; Wu, C. I.; Zhao, L. D.; Chung, D. Y.; Hogan, T. P.; Dravid, V. P.; Kanatzidis, M. G. High-performance tellurium-free thermoelectrics: all-scale hierarchical structuring of p-Type PbSe-MSe Systems (M= Ca, Sr, Ba). *J. Am. Chem. Soc.* **2013**, 135, 5152-5160.

(18) Liu, Y.; Yao, D.; Shen, L.; Zhang, H.; Zhang, X.; Yang, B. Alkylthiol-enabled Se powder dissolution in oleylamine at room temperature for the phosphine-free synthesis of copper-based quaternary selenide nanocrystals. *J. Am. Chem. Soc.* **2012**, 134, 7207-7210.

(19) Wibowo, R. A.; Jung, W. H.; Kim, K. H. Synthesis of $Cu_2ZnSnSe_4$ compound powders by solid state reaction using elemental powders. *J. Phys. and Chem. Solids* **2010**, 71, 1702-1706.

(20) Banu, I.; Rajagopalan, M.; Palanivel, B.; Kalpana G.; Shenbagaraman, P. Structural and electronic properties of SrS, SrSe, and SrTe under pressure. *J. Low Temp. Phys.* **1998**, 112, 211-226.

(21) Sobolev, V.; Merzlyakov, D. Sobolev, V. V. A study of the optical properties of barium selenide crystals. II. elementary transition bands and their fundamental parameters. *J. Appl. Spectrosc.* **2017**, 84, 255–260.

(22) Smet, P. F.; Moreels, I.; Hens Z.; Poelman, D. Luminescence in sulfides: a rich history and a bright future. *Materials* **2010**, 3, 2834-2883.

(23) Vercaemst, R.; Poelman, D.; Meirhaeghe, R. V.; Fiermans, L.; Laflere, W.; Cardon, F. An XPS study of the dopants' valence states and the composition of $CaS_{1-x}Se_x$:Eu and $SrS_{1-x}Se_x$:Ce thin film electroluminescent devices. *J. Lumin.* **1995**, 63, 19-30.

(24) Shin, J. S.; Kim, H. J.; Jeong, Y. K.; Kim, K. B.; Kang, J. G. Luminescence characterization of $(Ca_{1-x}Sr_x)(S_{1-y}Se_y):Eu^{2+}$, M^{3+} (M= Sc and Y) for high color rendering white LED. *Mater. Chem. Phys.* **2011**, 126, 591-595.

(25) Nazarov, M.; Yoon, C. Controlled peak wavelength shift of $Ca_{1-x}Sr_x(S_ySe_{1-y}):Eu^{2+}$ phosphor for LED application. *J. Solid State Chem.* **2006**, 179, 2529-2533.

(26) Zhang, X.; Liang, L.; Zhang, J.; Su, Q. Luminescence properties of $(Ca_{1-x}Sr_x)Se:Eu^{2+}$ phosphors for white LEDs application. *Mater. Lett.* **2005**, 59, 749-753.

(27) Game, D.; Ingale, N.; Omanwar, S. Synthesis and photoluminescence properties of Eu^{2+} doped CaS and SrS phosphor for phosphor converted white light emitting diodes. *J. Mater. Sci. Mater. El.* **2017**, 28, 915-922.

(28) Jia, D.; Wang, X. J. Alkali earth sulfide phosphors doped with Eu^{2+} and Ce^{3+} for LEDs. *Opt. Mater.* **2007**, 30, 375-379.

(29) Guo, C.; Huang, D.; Su, Q. Methods to improve the fluorescence intensity of CaS:Eu^{2+} red-emitting phosphor for white LED. *Mater. Sci. Eng. B* **2006**, 130, 189-193.

(30) Joos, J. J.; Van der Heggen, D.; Martin, L. I. D. J.; Amidani, L.; Smet, P. F.; Barandiarán, Z.; Seijo, L. Broadband infrared LEDs based on europium-to-terbium charge transfer luminescence. *Nat. Commun.* **2020**, 11, 3647.

(31) Kim, K. N.; Park, J. K.; Choi, K. J.; Kim, J. M.; Kim, C. H. Luminescent properties of $CaSe_{1-x}S_x$:Eu and application in LEDs. *Electrochem. Solid State Lett.* **2006**, 9, 262-264.

(32) Okada, D.; Nakamura, T.; Braam, D.; Dao, T. D.; Ishii, S.; Nagao, T.; Lorke, A.; Nabeshima, T.; Yamamoto, Y. Color-tunable resonant photoluminescence and cavity-mediated multistep energy transfer cascade. *ACS nano* **2016**, 10, 7058-7063.

(33) Nguyen, H. M.; Seitz, O.; Peng, W.; Gartstein, Y. N.; Chabal, Y. J.; Malko, A. V. Efficient radiative and nonradiative energy transfer from proximal CdSe/ZnS nanocrystals into silicon nanomembranes. *ACS nano* **2012**, 6, 5574-5582.

(34) He, Y. Q.; Zhang, M. Y.; Zhang, N.; Zhu, D. R.; Huang, C.; Kang, L.; Zhou, X. F.; Hu, M. H.; Zhang, J. Paper-based ZnS:Cu alternating current electroluminescent devices for current humidity sensors with high-linearity and flexibility. *Sensors* **2019**, 19, 4607.

(35) Achermann, M.; Petruska, M. A.; Koleske, D. D.; Crawford, M. H.; Klimov, V. I. Nanocrystal-based light-emittingm diodes utilizing high-efficiency nonradiative energy transfer for color conversion. *Nano Lett.* **2006**, 6, 1396-1400.

(36) Liu, C. Y.; Chen, T. P.; Kao, T. S.; Huang, J. K.; Kuo, H. C.; Chen, Y. F.; Chang, C. Y. Color-conversion efficiency enhancement of quantum dots via selective area nano-rods light-emitting diodes. *Opt. Express* **2016**, 24, 19978-19987.

(37) Wang, X. C.; Sun, J. L.; Dong, L.; Lv, C. F.; Zhang, K. K.; Shang, Y. Y.; Yang, T.; Wang, J. Z.; Shan, C. X. Stretchable and transparent electroluminescent device driven by triboelectric nanogenerator. *Nano Energy* **2019**, 58, 410-418.

(38) Xu, W. L.; Xu, W. L.; Wu, B.; Zheng, F.; Yang, X. Y.; Jin, H. D.; Zhu, F. Förster resonance energy transfer and energy cascade in broadband photodetectors with ternary polymer bulk heterojunction. *J. Phys. Chem. C* **2015**, 119, 21913-21920.

(39) Liu, Y. B.; Qiao, Y.; Sun, Z. C.; Zhang, W. G.; Liu, C. Y.; Wen, J. Y.; Liu, Y. Y.; Zhang, Q. Q.; Zhou Y.; Chen, J. Visual pressure interactive display of alternating current electroluminescent devices based on hydrogel microcapsules. *J. Mater. Chem. C* **2022**, 10, 12221-12231.

(40) Zuo, Y.; Shi, X.; Zhou, X.; Xu, X.; Wang, J.; Chen, P. Flexible color tunable electroluminescent devices by designing dielectric distinguishing double stacked emissive layers. *Adv. Funct. Mater.* **2020**, 30, 2005200.

(41) Dinh Xuan, H.; Timothy, B.; Park, H. Y.; Lam, T. N.; Kim, D.; Go, Y.; Kim, J.; Lee, Y.; Ahn, S. Il; Jin, S. H. Super stretchable and durable electroluminescent devices based on double network ionogels. *Adv. Mater.* **2021**, 33, 2008849.

(42) Zhao, C. B.; Yang, B.; Ali, M. U.; Zhao, Y. Q.; Zhang, C. H.; Yin, Y. M.; Liu, M.; Yan, C. Y.; Meng, H. Bright stretchable white alternating-current electroluminescent devices enabled by photoluminescent phosphor. *Adv. Mater. Technol.* **2022**, 7, 2101440.

(43) Tran, P.; Tran, P.; Tran, N. H.; Lee, J. H. Highly stretchable electroluminescent device based on copper nanowires electrode. *Sci. Rep.* **2022**, 12, 8967.

(44) Sun, Y. S.; Zhu, L. P.; Yang, J.; Zhang, J. J.; Chen, B. D.; Wang, Z. L. Flexible alternating-current electroluminescence plunging to below 1 Hz frequency by triboelectrification. *Adv. Optical Mater.* **2022**, 10, 2101918.

Table of Contents